Faraday Discussions

Unimolecular isomerisation of 1,5-hexadiyne observed by threshold photoelectron photoion coincidence spectroscopy

Journal:	*Faraday Discussions*
Manuscript ID	FD-ART-02-2022-000028
Article Type:	Paper
Date Submitted by the Author:	01-Feb-2022
Complete List of Authors:	Savee, John; ABB Inc, R&D Sztáray, Balint; University of the Pacific, Chemistry Hemberger, Patrick; Paul Scherrer Institut, Swiss Light Source Zádor, Judit; Sandia National Laboratories, Combustion Chemisty Department Bodi, Andras; Paul Scherrer Institute, Photon Science Department Osborn, David; Sandia National Laboratories,

Journal Name

ARTICLE TYPE

Cite this: DOI: 00.0000/xxxxxxxxxx

Unimolecular isomerisation of 1,5-hexadiyne observed by threshold photoelectron photoion coincidence spectroscopy †

John D. Savee,[‡a] Bálint Sztáray,[b] Patrick Hemberger,[c] Judit Zádor,[a] Andras Bodi,[c] and David L. Osborn*[a]

Received Date
Accepted Date

DOI: 00.0000/xxxxxxxxxx

The unimolecular isomerisation of the prompt propargyl + propargyl "head-to-head" adduct, 1,5-hexadiyne, to fulvene and benzene by the 3,4-dimethylenecyclobut-1-ene (DMCB) intermediate (all C_6H_6) was studied in the high-pressure limit by threshold photoelectron (TPE) spectroscopy. TPE spectra (TPES) were recorded with photoelectron photoion coincidence spectroscopy using synchrotron vacuum ultraviolet radiation. Reference TPES, obtained using pure compounds or judiciously extracted from the pyrolysis data, served as basis functions for pyrolysis quantification. From these spectra we measure a revised fulvene ionisation energy of 8.401 ± 0.005 eV. Temperature-dependent pyrolysis spectra were decomposed using these basis functions. The basis function coefficients were converted to product yields relying on assumed integral threshold photoionisation cross sections obtained by three, partially mutually exclusive sets of assumptions. Thus, the product yields of DMCB, fulvene, and benzene are established as well as their uncertainty. The derived mole fractions are consistent with modeling based on the C_6H_6 potential and RRKM master equation model of Miller and Klippenstein [*J. Phys. Chem. A*, 2003, **107**, 7783]. Although our results are fully consistent with parallel isomerisation pathways to benzene and fulvene found by Miller and Klippenstein, we observe the onset of fulvene at a lower temperature than the onset of benzene, in agreement with the master equation model but in contrast to the previous experiments of Stein et al. [*Proc. Combust. Inst.*, 1990, **23**, 85] This work promotes the use of photoion mass-selected threshold photoelectron spectroscopy as a rapid, sensitive, isomer-selective, and quantitative detection tool among the panoply of established analytical techniques.

1 Introduction

Isomerisation is a ubiquitous transformation in chemistry, playing critical roles in vision,[1] synthetic chemistry (e.g., enolisation[2] and sigmatropic[3] rearrangements), sugar synthesis,[4] atmospheric chemistry,[5,6] and soot formation.[7] Although Lindemann proposed his eponymous mechanism in 1922 to explain the kinetics and mechanism of unimolecular thermal dissociation reactions,[8] association and isomerisation reactions also derive their pressure-dependent rates from the same competition between collisional energy transfer and chemical reactions. Experimental studies of isomerisation on multi-well potential energy surfaces are more easily interpreted when conditions are chosen to be in the high-pressure limit. In this case, collisional equilibration is rapid compared to chemical change, and experimental results more directly reflect the enthalpy and entropy of barriers on the potential energy surface (PES), enhancing the ability to constrain and define models of PESs. However, experiments at lower pressures, in the fall-off region or the low-pressure limit, can also be valuable because they allow access to parts of the PES that are more difficult to reach when collisional stabilisation is too efficient. Therefore, experimental probes applicable over a range of pressures (and temperatures) can be an effective approach to study isomerisation mechanisms.

[a] *Combustion Research Facility, Sandia National Laboratories, Mailstop 9055, Livermore, California, 94551 USA, E-mail: dlosbor@sandia.gov*
[b] *Department of Chemistry, University of the Pacific, Stockton, California, USA.*
[c] *Laboratory for Synchrotron Radiation and Femtochemistry, Paul Scherrer Institute, 5232 Villigen, Switzerland.*

† Electronic Supplementary Information (ESI) available: Drawing of the pyrolysis reactor, pyrolysis TPES basis set reproduction and residuals, comparison of literature experimental and simulation results and the effect of residence time. See DOI: 00.0000/00000000.

‡ Present address: KLA Corporation, One Technology Drive, Milpitas, CA 95035, United States.

Unsaturated organic molecules offer an especially rich landscape for studies of isomerisation. The uncoupling and recoupling of π bonds allows a larger number of isomers—and lower energy pathways connecting them—than is possible in saturated molecular systems. One fascinating example is the isomerisation of C_6H_6,[9] with benzene being the most stable isomer. This system has been explored extensively since the first hypothesis that the reaction of two resonance-stabilized propargyl radicals ($HCCCH_2$) represents an important pathway for the formation of the first aromatic ring in the combustion of hydrocarbon fuels.[10,11] Considering the molecular structure of propargyl, it is highly unlikely that the recombination of two could yield benzene in an elementary reaction step. Instead, the two terminal carbons of propargyl each have substantial unpaired electron density, leading to three possible acyclic adducts that can form upon recombination of this asymmetric free radical. Of these, the "head-to-head" recombination pathway yields 1,5-hexadiyne (1,5-HD), the least stable of the three possible adducts, as shown in Scheme 1:

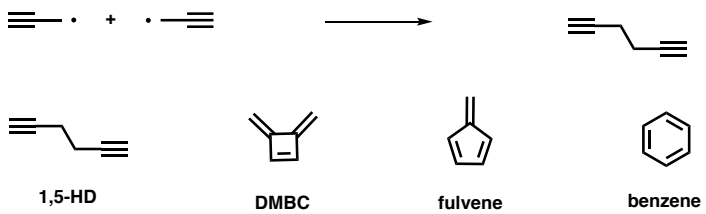

The most complete theoretical investigation of the propargyl self-reaction is from Miller and Klippenstein (MK),[12] who calculated stationary points on the PES using high-level electronic structure methods. They extracted rate coefficients for numerous elementary reactions on the C_6H_6 surface by solving an RRKM-based master equation, treating both collisional energy transfer and chemical kinetics. A key experimental study to which they validated their theoretical treatment was performed in 1990 by Stein et al.,[13] who heated 1,5-HD in a flow reactor and observed its conversion to 3,4-dimethylenecyclobut-1-ene (DMCB), fulvene, and benzene (Scheme 1). They separated isomers at each temperature using gas chromatography, and observed the products with flame ionisation, mass spectrometry, and infrared spectroscopy. Using radical scavengers and radical sources, they found no evidence for the participation of free radicals in the isomerisation process. For systems like this, where isomerisations happen on a singlet PES, slow separation and detection techniques (minutes to hours), as used by Stein et al.,[13] can provide accurate results if no further chemistry takes place during separation and detection. However, for isomerisations on a doublet PES, as in the addition of radicals to unsaturated molecules (e.g., OH + CH_3CHCH_2),[14] much faster methods for isomer-resolved chemical analysis are needed.

Photoionisation mass spectrometry (PIMS) using single-photon ionisation by tunable vacuum ultraviolet radiation is a rapid method for such studies.[15–17] Neutral isomers are selectively identified and quantified at a single mass-to-charge (m/z) ratio by their distinct ionisation energies (IEs) and photoionisation spectra. A more detailed molecular fingerprint can be obtained by photoelectron photoion coincidence (PEPICO) spectroscopy,[18–22] in which photoelectron spectra can be extracted for each m/z channel, i.e., photoion mass-selected (threshold) photoelectron spectra (ms-TPES), to distinguish isomers.[23,24] To demonstrate the utility of this approach for the study of isomerisations, we use PEPICO spectroscopy in this work for the rapid analysis of the previously explored 1,5-HD system. The certainty of isomeric assignments from ms-TPES significantly exceeds that of PIMS for these rigid, cyclic species. The gradual change of spectra as a function of temperature can be used to extract reference spectra of single isomers observed in this system. The reference spectra we measure for DMCB and fulvene represent the most-resolved TPES available for these species. Together with measured or estimated (integral threshold) photoionisation cross sections of the individual isomers, we probe the reaction progress by extracting mole fractions of the C_6H_6 isomers at each temperature. Although our findings are largely in agreement with the earlier work of Stein et al.,[13] we find that fulvene arises at a lower temperature than the more stable benzene isomer, which reflects details of the underlying PES and agrees with the master equation simulations of Miller and Klippenstein.[12] In addition, we show that isomers can be reliably quantified using ms-TPE spectroscopy, with potential applications in complex reaction mixtures relevant to combustion, catalysis and astrochemistry.

2 Experimental Methods

The imaging PEPICO (iPEPICO) apparatus located at the Paul Scherrer Institute (PSI) was described in detail previously,[25,26] and only a brief summary of the instrument with a more detailed description of the new pyrolytic reactor system is provided here. Synchrotron radiation from the bending magnet VUV beamline of the Swiss Light Source was collimated with a platinum-coated copper mirror before entering a turntable-style grazing incidence monochromator.[18] In the experiments presented here, the 600 lines mm^{-1} laminar silicon grating was used, as it is best suited for high resolution experiments between photon energies of 7 and 14 eV. To suppress higher order radiation of the grating, the dispersed light was focused and directed into a differentially pumped gas filter, filled over an optical length of 10 cm with a 10 mbar mixture of 60% Ne, 30% Ar, and 10% Kr. The photon energy was calibrated using autoionisation lines of argon and neon in first and second order, confirming a photon energy resolution of 3 meV at 10 eV.

Samples were introduced either through a simple effusive, unheated inlet or, for in-situ pyrolysis, through a newly designed heatable borosilicate reactor. The vapor from a commercial liquid sample of 1,5-HD in pentane (50:50 mixture) was diluted to 5% concentration in argon. A mass flow controller regulated the flow of this mixture at 0.25 sccm into the heatable reactor. The reactor (Fig. S1†) had 4

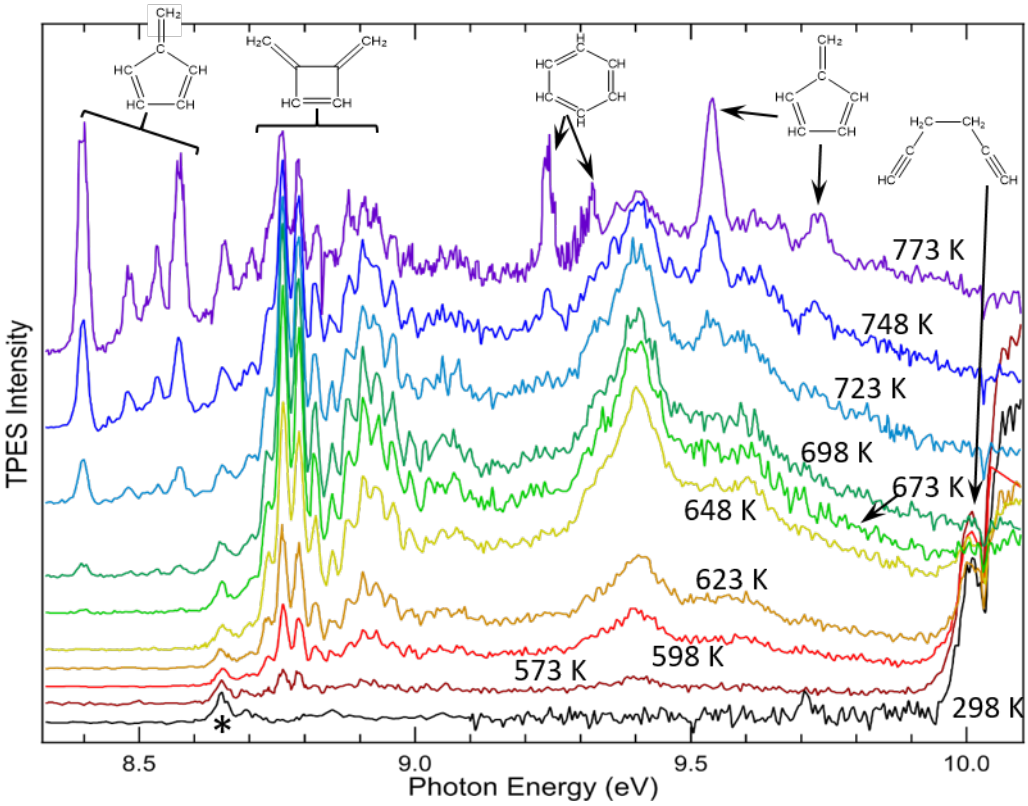

Fig. 1 Threshold photoelectron spectra as a function of 1,5-hexadiyne pyrolysis temperature. The most diagnostic spectral features for each C_6H_6 isomer are labeled, and the main band of the impurity, Z/E-13HD5Y is indicated by an asterisk.

mm internal diameter (ID) with a 32 mm long heated zone. Immediately after this zone the ID narrowed to a 0.1 mm capillary section within a 2 mm long transition. This design provides constant, slow flow velocity ($\sim$2.7 mm s^{-1}) in the 4 mm ID section followed by rapid flow in the capillary portion, which quickly sweeps the flow into the high vacuum chamber for analysis. Four heating cartridges (Watlow FIREROD with 150 W heating power each) were contained in a copper block, which encircled the reactor over the heated length. A type K thermocouple was used to measure the reactor surface temperature at the midpoint of the heated zone and control the heating via a Eurotherm 3216 PID controller. The gas pressure in the reactor varied from 0.24 to 0.42 bar. Given our measured temperatures (295–773 K), flows, and pressures, the calculated residence time in the heated zone varied from 9.5 to 14.2 s, with an average of 11.8 s. Expansion from the capillary into the high vacuum of the ionisation region of the iPEPICO spectrometer suppressed collisions abruptly, stopping all further chemistry before the sample was intersected by the VUV synchrotron radiation with a 4×4 mm^2 spot size. Pressure in the ionisation chamber was kept at 5×10^{-6} mbar, regulated by the flow of the 1,5-HD/argon mixture.

Ions and electrons produced after VUV photoionisation were extracted from the ionisation region in a constant 120 V cm^{-1} electric field. In a grid-less setup, photoelectrons were velocity map imaged based on their off-axis momentum onto a Roentdek DLD40 position sensitive delay-line detector. The electron optics focused the zero kinetic energy (threshold) electrons in a small center spot with better than 1 meV resolution. However, energetic electrons with a momentum exactly parallel to the flight tube axis are also imaged to this spot, and contribute to the "hot" electron background signal. Subtracting the contribution of these hot electrons was based on the signal in a ring region around the center spot, as proposed by Sztáray and Baer.[27] Photoions were mass analyzed using a two-grid Wiley–McLaren-type linear TOF setup and detected on a Chevron-stack of multichannel plates in a Jordan TOF C-726 non-imaging detector in the multiple-start/multiple-stop delayed coincidence data acquisition scheme.[28] Photoelectron and photoion detection events served as start and stop signals for the cation TOF analysis, respectively.

Coincidence count rates between threshold electrons (corrected for the effect of hot electrons, vide supra) and photoions with a time of flight corresponding to m/z 72 were plotted as a function of photon energy between 8.3 and 10.1 eV. We saw no contributions of other cation mass channels to the threshold photoelectron signal in this energy range, which is why, instead of the ms-TPES, the total threshold photoelectron spectra with better signal-to-noise ratios are shown at room temperature and in a 573-–773 K temperature range of the pyrolytic reactor in Fig. 1.

3 Theoretical Methods

The temperature-dependent threshold photoelectron spectra were interpreted in two steps. First, a basis set was constructed consisting of reference C_6H_6 TPE spectra for the isomeric spectral carriers. These are 1,5-HD, DMCB, fulvene, benzene, and a contaminant, identified as 1,3-hexadien-5-yne (Z/E-13HD5Y, also known as 1-ethynyl-1,3-butadiene, see below and in Fig. 2). Franck–Condon factors were calculated in the double harmonic approximation including Duschinsky rotations at an assumed vibrational temperature of 350 K at the B3LYP/6-311++G(d,p) level of theory using Gaussian 16.[29] Time-dependent density functional theory was used to simulate the first excited state band for fulvene. For DMBC, this could be achieved using the equation of motion formalism for ionisation energies with coupled cluster singles and doubles,[30] i.e., EOM-IP-CCSD/cc-pVDZ calculations with Q-Chem 4.3.[31] The FCFs were convolved with a 15–30 meV FWHM Gaussian distribution to account for the rotational envelope and the instrumental resolution to produce a spectral simulations. Adiabatic ionisation energies were calculated using the G4 composite method.[32] We also calculated vertical ionisation energies at the EOM-IP-CCSD/cc-pVTZ//B3LYP/6-311++G(d,p) level. In order to understand the difficulties modeling 1,5-hexadiyne spectra, we optimized the cation geometries using EOM-IP-CCSD/cc-pVDZ, which revealed large geometry changes between the neutral and the $\widetilde{\mathbf{X}}^+$ ^{2}B state of the *gauche* conformer by internal rotation.

We solved the master equation using the Variflex v.2.03 code.[33] The molecular data (geometries, harmonic frequencies, hindered rotors, energies, and tunneling parameters) were identical to these parameters used by Miller and Klippenstein.[12] As stated in their paper, the C_6H_6 system is in the high-pressure limit above 67 mbar in this temperature range. Because all our reactor pressures were higher than this value, we used the high-pressure limit rate coefficients in our simulations. The kinetic ODE was solved[34] by the SciPy Python package's ODE integrator that uses lsoda from the Fortran library odepack. The residence time in the heated region of the reactor was determined based on the flow velocity $v = \dot{q}_0 \frac{p_0 \cdot T}{p \cdot T_0 \cdot A}$, where $\dot{q}_0$ is the standard volumetric flow rate at a pressure and temperature of p_0 and T_0, respectively, A is the reactor cross sectional area, and p and T are the experimental pressure and temperature. The maximum, average, and minimum residences used in our experiments were found to be 14.5, 11.8, and 9.5 s, respectively, which were used to integrate the system to calculate the yields. As discussed below, we adjusted one barrier height by 1.0 kcal mol^{-1} to improve agreement with the experiment. This adjustment is within the estimated uncertainty of the high-level electronic structure methods used by Miller and Klippenstein.

4 Results

Fig. 1 shows the TPE spectra from pyrolysis of a flowing gas phase 1,5-hexadiyne / pentane sample in argon over the temperature range 298–773 K. Although we do not know the ratio of 1,5-HD to pentane in the gas phase, it is unlikely that thermal decomposition of pentane would generate any C_6H_6 products, and therefore should not affect our conclusions. At 298 K, the TPE spectrum is dominated, as expected, by 1,5-HD, with an onset near 9.95 eV, consistent with the reported photoelectron spectrum of Brogli et al.,[35] who measured an ionisation energy (IE) of 9.90 eV. The impurity denoted by an asterisk is discussed in section 4.1.

As we increased the temperature, the spectra were unchanged until ∼573 K. Above this temperature the spectra gradually evolve as 1,5-HD isomerizes. The spectra reveal the presence of three additional C_6H_6 isomers, with the most characteristic peaks for isomeric assignment denoted in Fig. 1. We attempted to collect a spectrum at 798 K, but the capillary portion of the reactor became clogged with carbonaceous particles, preventing experiments at higher temperatures. To extract mole fractions of C_6H_6 isomers vs. temperature, we fit a linear combination of reference spectra for each isomer to the data in Fig. 1, and scale each fit coefficient by assumed integral TPES cross sections, as described in the sections below.

4.1 Reference TPES

Reference TPE spectra for C_6H_6 isomers could be measured for pure 1,5-HD and benzene. Unfortunately, pure samples of the other isomers are not commercially available. Fortunately, the gradual change of spectra with temperature seen in Fig. 1 makes it possible to extract the remaining required reference spectra from these data. The black traces in Fig. 2 show experimental TPE spectra for the C_6H_6 isomers determined in the present work. The results of Franck–Condon factor (FCF) calculations for ionisation from the ground state of the neutral species to the ground and excited electronic states of the corresponding cation are shown in blue and orange, respectively. The simulated spectra were shifted along the photon energy axis to align the calculated origin transitions with experiment, where the former came from G4 calculations with an estimated uncertainty of 50 meV.

The TPE spectrum for 1,5-HD was measured by passing the sample mixture through the effusive inlet at room temperature. The resulting TPE spectrum, shown in Fig. 2(a), is not perturbed by pentane (m/z 72, IE = 10.36 eV)[36] and is in good agreement with the reported IE for 1,5-HD, 9.90 eV.[35] The simulation of the 1,5-HD photoelectron spectrum is fraught with challenges. The *antiperiplanar* and *gauche* conformers are almost isoenergetic and have comparable abundances at room temperature. The ground and first two excited electronic states are computed to have vertical ionisation energies below 10.6 eV using EOM-IP-CCSD. Also according to EOM-IP-CCSD calculations, the $\widetilde{\mathbf{X}}^+$ ^{2}B ground state of the C_2 *gauche* conformer undergoes large internal rotation, associated with 0.4 eV stabilisation from the neutral geometry. Therefore, the 1,5-HD TPES cannot be simulated in the double harmonic approximation and is likely also affected by coupling between close-lying electronic states. Consequently, we are not reporting attempts to model the 1,5-HD TPES. A minor C_6H_6 impurity was observed in the 1,5-HD sample with an origin transition near 8.65 eV (Fig. 2(b)). After consideration of

several C_6H_6 isomers, we assign this contaminant as 1,3-hexadien-5-yne. Rosenstock et al.[37] estimated the IE of 13HD5Y as 9.2 eV based on corrected electron ionisation measurements. Nonetheless, our calculated IEs for E-13HD5Y (8.67 eV) and Z-13HD5Y (8.71 eV) and the agreement of the associated FCF simulation with the TPE spectrum for the impurity strongly support our assignment. The first two peaks are characteristic of the E/Z isomer distribution, and the TPES could be fit assuming $\sim$ 20% Z and 80% E isomer, which is somewhat different from the ab initio equilibrium prediction of 50–50% with the two isomers being practically isoenergetic at G4 level of theory. Note that the IE of 1,2,4,5-hexatetraene (1245HT) was measured by Bischof et al. as 8.53 eV,[38] and there is no evidence for the presence of this isomer in any of our spectra.

As temperature increases from 573 to 673 K, the spectral features in the 8.7–9.9 eV energy range in Fig. 1 increase at the same rate, consistent with the increasing contribution of a single new isomer. Having already identified the reference spectra of 1,5-HD and the impurity 13HD5Y, we subtract these two contributions from the 673 K spectrum, yielding a flat baseline near 8.65 eV and no sign of the sharp rise of 1,5-HD near 10.0 eV. The resulting TPE spectrum is shown in Fig. 2(c). We assign this spectrum to the C_6H_6 isomer DMCB. Its literature IE of 8.80 eV[39] agrees with our G4 value of 8.80 eV, and our FCF simulation also supports this assignment up to $\sim$ 9.1 eV. Above this photon energy, the TPE spectrum is characterized by a significant amount of unresolved signal and a broad peak centered at $\sim$ 9.45 eV. Our EOM-IP-CCSD/cc-pVDZ calculations predict vertical ionisation to the $\widetilde{\mathbf{A}}^+\ ^2A_2$ first excited state of the C_{2v} DMCB at 9.40 eV, which agrees with the position of this broad peak also reported by Heilbronner et al.[39] We calculated a FC simulation based on the optimized EOM-IP-CCSD geometry of the $\widetilde{\mathbf{A}}^+\ ^2A_2$ state, which agrees well with the weak features appearing above 9.4 eV. However, the vibrational structure in the first excited state may be lost due to lifetime broadening, as was also observed in the fulvenone TPES.[40] In an important contrast to the benzene and fulvene spectra discussed below, which exhibit negligible baselines, the DMCB TPES starts to deviate from the ground-state FCF model above 9.0 eV. This extra signal may arise from coupling between the lowest two cation electronic states, which our calculations show are quasi-degenerate at the optimized geometry of the first excited state. Such strong coupling could also facilitate autoionisation of the Rydberg states formed promptly after photoabsorption. We tentatively assign the broad unresolved signal as evidence for autoionisation, which may lead to an overall increase of the integrated TPES intensity as well.

The TPE spectrum for benzene, shown in Fig. 2(d), was obtained using a pure benzene sample introduced to the ionisation chamber through the effusive inlet. The origin transition is centered at 9.241 eV, i.e., 3 meV lower than the known IE of 9.24384(6) eV.[41] The 3 meV red-shift of the peak maximum is likely the result of broadening due to the Stark shift in the constant extraction field.[42] Moreover, the spectrum measured in the present work is nearly identical to the one measured by Yencha et al.[43] and the FCF simulation for benzene is in reasonable agreement with the experimental spectrum.

Starting at 673 K, the first sign of a new isomer can be seen from a peak at 8.398 ± 0.005 eV, which rises from a very low-noise baseline. This peak is consistent with the C_6H_6 isomer fulvene, whose IE was measured by Heilbronner et al.[39] as 8.36 eV. We extract the TPE spectrum of fulvene from the 773 K spectrum in Fig. 1. At this temperature, 1,5-HD does not contribute to the TPE spectrum, but features from DMCB and benzene remain. The benzene TPE spectrum in Fig. 2(d) was used to subtract signal from the 773 K data until the defining benzene peak at 9.241 eV disappeared into the the broader baseline. Then, the DMCB TPE spectrum in Fig. 2(c) was subtracted from the remaining 773 K spectrum until there was approximately zero signal in the vicinity of the DMCB peak near 9.4 eV. We assign the resulting spectrum in Fig. 2(e) to fulvene based on the good agreement with the Heilbronner spectrum,[39] which was acquired from a synthesized fulvene sample, and the excellent agreement with our FCF simulation near the first ionisation energy. The progression of resolved features beginning at 9.55 eV are consistent with the features observed by Heilbronner et al.[39] and are assigned to ionisation into the $\widetilde{\mathbf{A}}^+\ ^2B_1$ excited electronic state of C_{2v} fulvene. Fig. 2(e) also shows a Franck–Condon simulation of this state, obtained with TD-DFT calculations, which shows excellent agreement with the observed signal. Based on these results and taking into account the red shift of the benzene 0–0 peak maximum with respect to the true ionisation energy, we propose a revised fulvene ionisation energy of 8.401 ± 0.005 eV.

4.2 From fit coefficients to product yields

The ionisation energy calculations and FCF simulations helped us understand the TPES structure and increased our confidence in the experimentally derived reference TPES. The experimental pyrolysis TPES as a function of temperature (Fig. 1) were then decomposed into contributions from each isomer using the normalized reference TPES as basis functions (Fig. 2). The basis function coefficients for the normalized reference spectra were obtained by minimizing the sum of squared differences between the sum spectra plus a constant baseline and the normalized temperature-dependent experimental TPES. On average, the sum of coefficients was 1.07, i.e., close to unity. The residuals were on the order of the signal-to-noise ratio of the spectra, as shown for the 748 K spectrum in Fig. 3. Fits for all temperatures are shown in Fig. S2.[†] The results of the basis set reconstruction are shown in Fig. 4(a). We disregarded the 13HD5Y contaminant's coefficients (which were never more than a few percent for $T > 298$ K) and set the benzene and fulvene coefficients to zero below 698 K and the 1,5-HD coefficients to zero above 673 K. In these temperature ranges, the fitted coefficients for these reference spectra were, on average, ± 0.005, as they have negligible contributions to the measured spectra. The main assumption in this decomposition is that the TPES of the C_6H_6 isomers are either independent of the temperature in the studied range or that there was sufficient collisional cooling in the borosilicate capillary in the $\sim$ 5 ms the flow passed it, in the expansion into the ionisation chamber, or with the ionisation chamber walls to ensure that the sample is ionized at $\sim$ room temperature. This assumption was validated by the

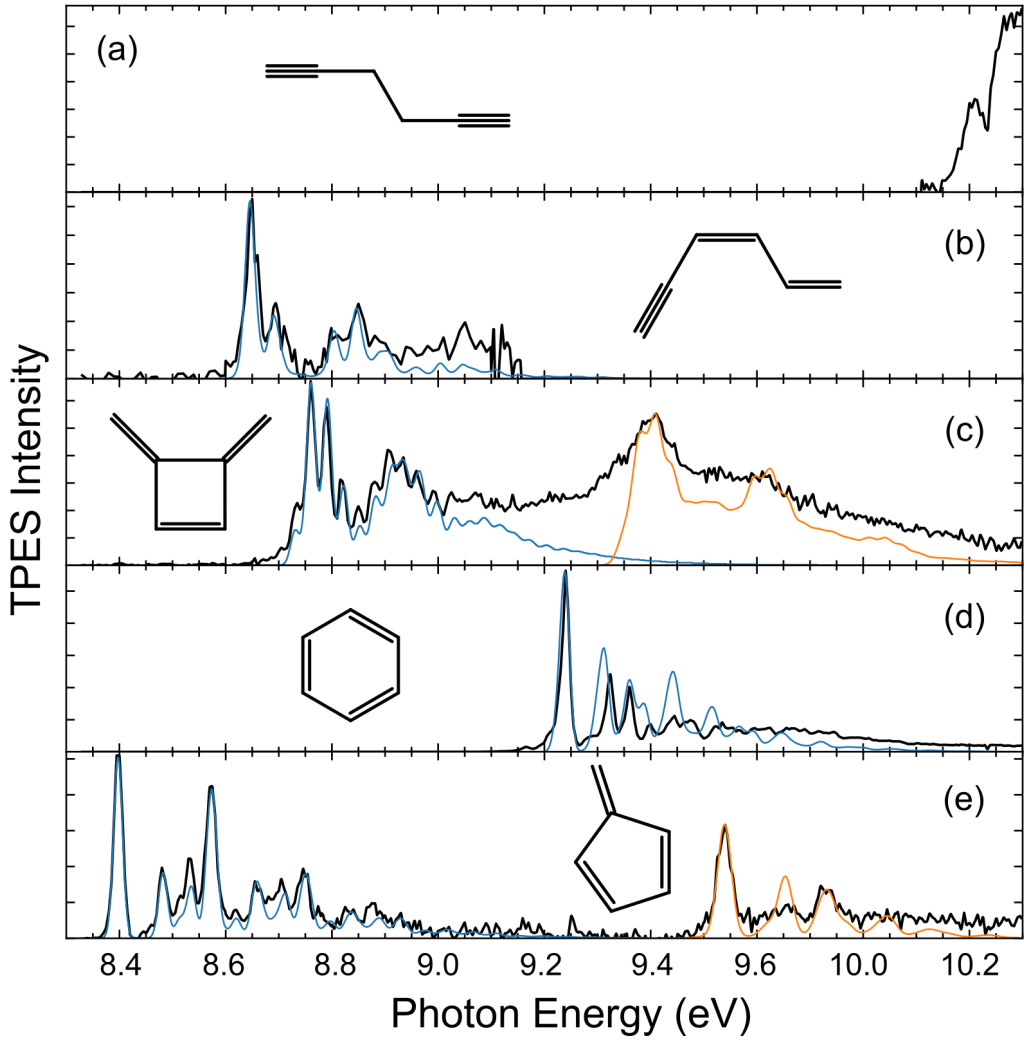

Fig. 2 Spectra of the five individual isomers of C_6H_6. (a) 1,5-HD, (b) 13HD5Y, (c) DMCB, (d) benzene, and (e) fulvene. The spectra in (a)–(c) and (e) were extracted from the 1,5-HD sample at appropriate temperatures from data in Fig. 1. Spectrum (d) is from an authentic sample of benzene. Franck–Condon simulations of ionsation to the ground and first excited electronic states of the cations are shown in blue and orange, respectively.

fact that experimental spectra were reproduced very well at all temperatures by the basis set decomposition, even though the reference spectra are derived from data at only a few temperatures. However, the resulting reference TPES coefficients are not equal to the relative product yields. The TPES intensities, and therefore the reference TPES coefficients, are linearly dependent on the number densities of the species in the ionisation region, thus, barring sampling effects, they are proportional to the concentration of each component. The proportionality constant is related to the (integral) threshold photoionisation cross section of each isomer in the reference energy range, which may vary among isomers.

In the second step, we need to convert the basis set coefficients to relative abundances, most importantly for DMCB, fulvene, and benzene. We first define integral threshold photoionisation cross sections (iTPICS) as the integral of the threshold photoionisation cross section, which is proportional to the threshold photoelectron signal, over the photon energy range of interest, on a per molecule basis. As iTPICS are unknown, we propose three scenarios to estimate their relative values and convert the C_6H_6 reference TPES basis set coefficients to product yields. The first scenario assumes that the integral threshold photoionisation cross section of the three isomers is the same in the 8.3–10.1 eV energy range. Justification for this assumption is given below. Furthermore, this energy range completely encompasses two cation electronic state bands in DMCB and fulvene, as well as the doubly degenerate ground state band of benzene. In the second scenario, we consider the effects of the raised DMCB TPES baseline (see Fig. 2c) on the intensities. In the third scenario, we note that photoionisation spectra have been proposed to be loosely related to the integral of the photoelectron spectrum.[44,45] We therefore estimate the photoionisation cross section of these three isomers at 10 eV and assume that their integral TPES intensity corresponds to these. Based on these scenarios, we propose an uncertainty range for the mole fractions of the C_6H_6 isomers as a function of reactor temperature.

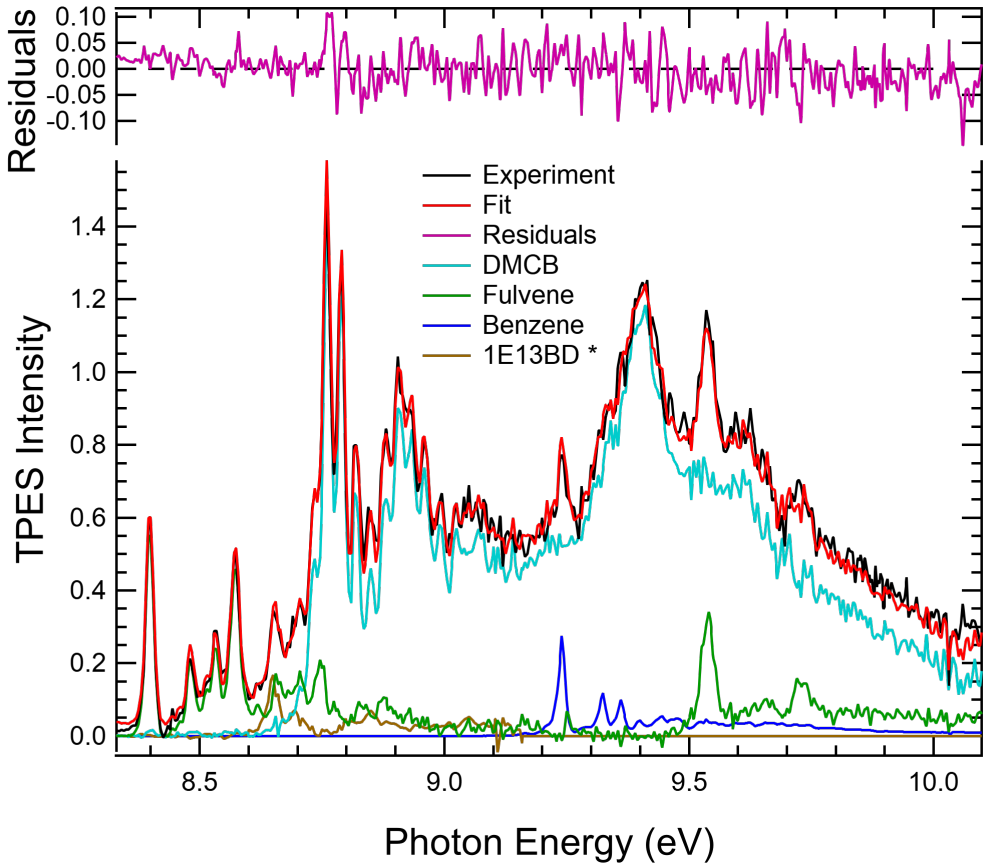

Fig. 3 Fit of the spectra at 748 K to a linear combination of C_6H_6 isomer threshold photoelectron spectra. The TPES basis functions for each isomer are shown along with the fit residuals at the top. Analogous fits are provided for all temperatures in Fig. S2 of the ESI.†

DMCB is seen at the majority of temperatures, so we chose a unity factor for its basis function coefficient. Only 1,5-HD and DMCB coexist at low temperatures. Total ion signal at both 10.365 and 10.890 eV were reduced by a factor of 2 at 673 K compared to 523 K. This reduction with increasing temperature may be due to the larger ionisation cross section of 1,5-HD compared to DMCB at these energies, as well as to temperature-dependent sampling effects. A 1,5-HD basis function coefficient of 8 restores this overall intensity drop as far as the total abundance is concerned in the temperature-dependent TPES. It is also reasonable considering that the reference TPES for 1,5-HD contains only a small part of the first TPES band in Fig. 2(a), whereas two electronic states are fully contained in the DMCB reference in Fig. 2(c). Furthermore, the 1,5-HD photoionisation cross sections may be enhanced compared to all other species because of the presence of its triple bonds.[46] Yet this factor of 8, used in all three scenarios, is the least-well defined isomer factor and affects the position and, to a lesser extent, shape of the 1,5-HD disappearance and the DMCB appearance in the isomerisation mole fraction diagram in Fig. 4(b). If it is changed from 5 to 15, the crossover temperature of 1,5-HD/DMCB moves from 625 to 650 K, which gives some indication of the uncertainty of the low-T product yield results.

Two cation electronic states are fully included in the reference TPES of DMCB, fulvene and benzene. The HOMO and HOMO−1 orbitals in the neutrals correspond to similar π bonding orbitals in all three, which suggests that both the transition dipole moments and the integrated FCF over the whole bands will be similar. Therefore, as long as the dipole and the sudden approximations hold for the ionisation mechanism, or deviations from them cancel out, the total TPES intensities integrated over the first two bands in the 8.3–10.1 eV region (including the degenerate $\widetilde{\mathbf{X}}^+\ ^2E_{1g}$ ground state of the benzene cation in D_{6h}), should be the same for the three C_6H_6 isomers. The first scenario therefore uses unity basis function coefficients for benzene, fulvene, and DMCB.

In the second scenario, we note that the lowest 200 meV of the DMCB TPES in Fig. 2(c) is almost perfectly reproduced by the FCF calculations, but the spectrum does not return to negligible baseline and instead exhibits a large and almost constant signal up to 9.6 eV, on top of which sits the $\widetilde{\mathbf{A}}^+\ ^2A_2$ excited state peak at 9.4 eV. The enhanced threshold photoionisation signal may be due to Rydberg-state mediated autoionisation and the strong coupling between the $\widetilde{\mathbf{X}}^+\ ^2B_1$ and $\widetilde{\mathbf{A}}^+\ ^2A_2$ states.[40] As a consequence, the threshold photoionisation efficiency (i.e., the quantum yield for threshold ionisation) may be higher in DMCB than in fulvene and benzene, leading to a larger TPES integral cross section. Between 8.65 and 9.30 eV, i.e., below the onset of the excited state peak, the TPES intensity is 1.3× higher than that of the FC simulation if the latter is fitted to reproduce the vibrational intensities below 9.0 eV. This apparently enhanced DMCB signal led us to propose a conservative estimate in the second secenario that the DMCB TPES integral

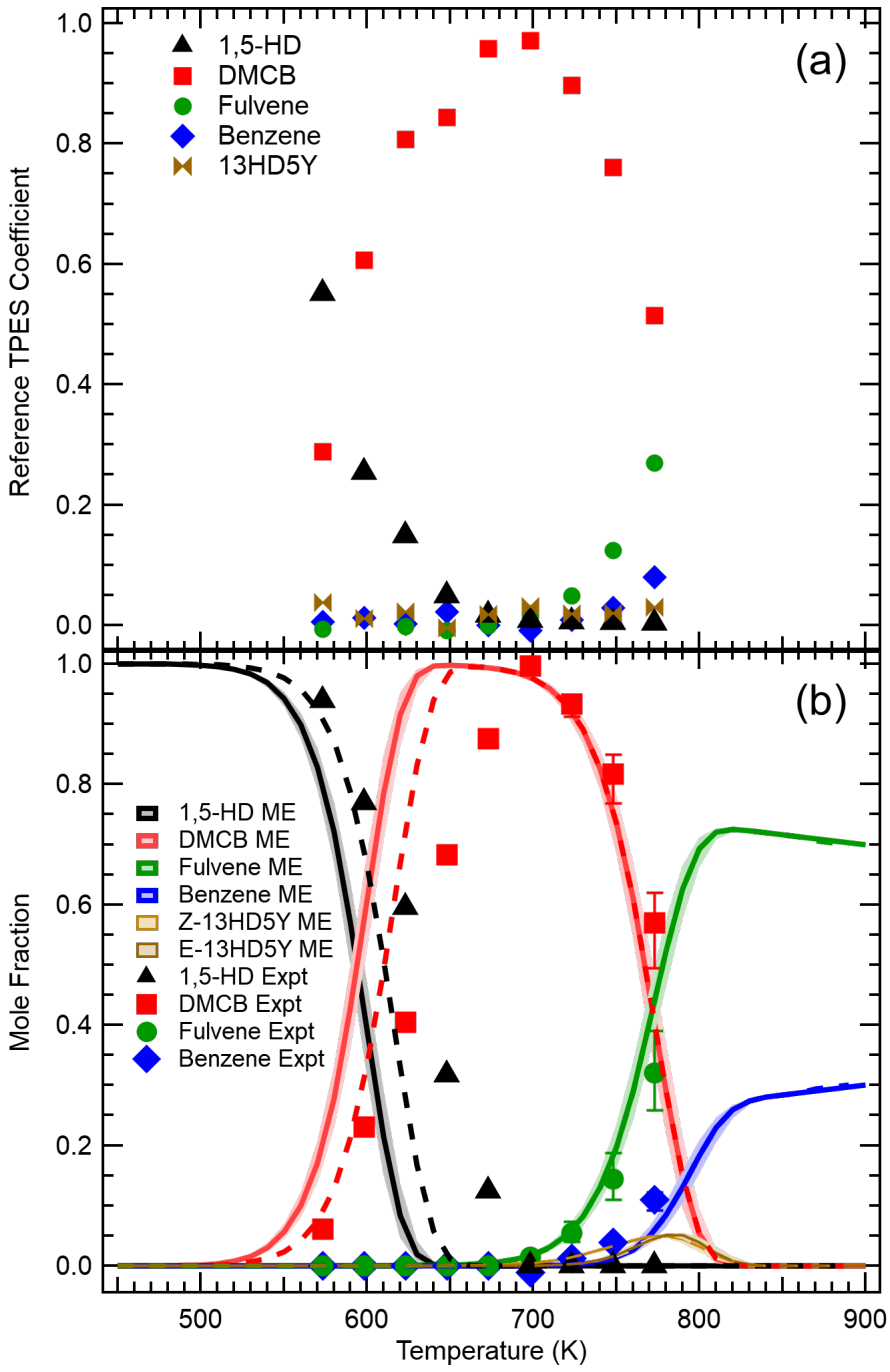

Fig. 4 (a) Coefficients for the C_6H_6 isomer reference TPES are shown as a function of the reactor temperature in 1,5-hexadiyne pyrolysis. They are converted to abundances and the isomer product yields shown in (b) using three scenarios with the working assumptions to obtain the relative integral threshold photoionisation cross sections described in the text. Experimental (symbols) error bars represent the range of results based on the three scenarios (see text). Solid lines show the master equation simulation at the average 11.8 s residence time, with shading showing limits of simulations at 9.5 to 14.5 s residence times. Dashed lines show the ME simulation for 11.8 s residence time with barrier connecting wells 1 and 2 increased by 1.0 kcal mol^{-1}.

cross section is 1.5× larger than that for fulvene and benzene.

Scenario three is based on the assumed quasi-equivalence of the integral photoelectron spectrum with the photoionisation spectrum. Consequently, the integral threshold photoelectron signal should be proportional to the photoionisation cross section (PICS).[44,45] Benzene, fulvene, and DMCB are all rigid structures with 6 π electrons. They have two cation electronic states each below 10 eV. Soorkia et al. also reported fulvene and DMCB photoionisation spectra in 2010.[47] Based on these, we can assume that the absolute photoionisation cross section of these three C_6H_6 isomers will be very similar at equal excess energies above the ionisation energy. The benzene PICS at 10 eV is known to be 23.4 Mb.[48] For fulvene, 10 eV photon energy is 1.60 eV above the IE. The same excess energy in benzene corresponds to 10.88 eV photon energy, at which the benzene PICS is 38.6 Mb. DMCB has a higher ionisation energy of 8.80 eV, which implies that its PICS at 10 eV should be equal to that of benzene at 10.44 eV, i.e., 30.5 Mb. Thus, the assumed DMCB : fulvene : benzene PICS at 10 eV of 30.5 : 38.6 : 23.4 Mb imply scaling factors of 1.00 : 0.79 : 1.30, respectively, to convert the TPES basis function coefficients into mole fractions.

The basis set coefficients shown in Fig. 4(a) were converted to product yields according to the three scenarios. The average mole fractions are plotted in Fig. 4(b) together with error bars for the DMCB, fulvene, and benzene data corresponding to the product yield range spanned by the results.

4.3 Master equation results

We solved the master equation in the high-pressure limit for a model of the PES defined by the stationary points shown in Fig. 5, using electronic structure results of MK.[12] Our first solution of the master equation for thermal isomerisation of 1,5-HD utilized a 30-second residence time of molecules in the heated zone in order to reproduce the calculations of MK[12] and compare with the earlier experimental results of Stein et al.[13] that used this residence time. These calculations reproduce nearly exactly the previous ME results, as shown in Fig. S3.† The ME results shown as solid lines in Fig. 4(b) are calculated at our average experimental residence time of 11.8 s, with shading showing the ME predictions for our shortest (9.5 s) and longest (14.5 s) residence times, which varied across our experimental datasets. The dashed lines show our predictions when the energy of the **1–2** saddle point in Fig. 5 is increased by 1.0 kcal mol^{-1}.

5 Discussion

In their 2003 paper on the propargyl radical self-reaction, Miller and Klippenstein[12] stated that "...the low-temperature isomerisation experiments [of Stein et al.][13] are a fairly direct test of the most important features of the [C_6H_6] PES..." Given the high sensitivity of chemical kinetics to saddle point energies, MK made slight adjustments to barriers **1–2** and **2–3** (see Fig. 5) in order to improve agreement with the Stein et al. data. Part of our motivation was to provide additional data using a complementary and more direct experimental method for comparison with theoretical predictions. We now discuss the two experimental datasets and their connection to the underlying PES depicted in Fig. 5.

5.1 Comparison between experiments

At a qualitative level, our results are in good agreement with the experiments of Stein et al., showing the conversion of 1,5-HD to DMCB with increasing temperature, followed by the production of fulvene and benzene at higher temperatures. Looking more closely, there are three main differences between our experiments and those of Stein et al. (see Fig. S4 for a direct comparison).† First, with increasing temperature, their loss of 1,5-HD and rise of DMCB occur at lower temperatures compared to our data, which could simply reflect their $\sim$ 3x longer residence time. However, the shift of their profiles with respect to ours is less dramatic at higher temperatures, where DMCB is consumed as fulvene increases. For the production of benzene, our profiles are nearly the same as theirs, despite the difference in residence times. The second difference is the fact that Stein et al. observe a fairly flat profile of DMCB, with 97% or greater yield from 620 to 720 K, whereas our DMCB profile peaks more sharply at 698 K. The third, and most important difference is that the data of Stein et al. show the first observations of both fulvene and benzene at the same temperature, 736 K. By contrast, our data shows evidence of fulvene at 673 K, with quantifiable amounts starting at 698 K, whereas benzene first appears at 723 K. Before considering how these differences may affect our understanding of the PES, we consider four potential sources of experimental systematic errors.

First, Stein et al. used "a steady 20 cm^3 min^{-1} flow (at room temperature and 1 atm)" with a reactor pressure of 1 atm and "residence times near 30 seconds." Molar flow, pressure, and residence cannot all be constant when gas temperature is varied. Because constant molar flow is straightforward to maintain, and pressure gradients are difficult to maintain, it seems most likely that over their temperature range of 523–823 K (a 57% increase in absolute temperature), their residence time decreased by 36%, whereas MK used a constant 30 s residence time in their modeling of the Stein experiments. Nevertheless, the ramifications of this likely mismatch between experimental and modeled residence times is not significant compared to the scatter in Stein's experimental data. A comparison can be seen in Fig. S5,† which shows reducing modeled residence times from 30 s to 11.8 s (a 61% decrease) generates a shift of all mole fraction profiles by 20 K to higher temperature.

Stein et al. quote a temperature uniformity of 2 K throughout the volume of their 10 mm ID reactor. Although they don't say where temperature was measured, it is reasonable to believe their transducer was in direct contact with the gas given the relatively

large diameter of their reactor, and therefore likely accurate. In contrast, we measured the temperature of our 4 mm ID reactor only on the external surface, and this temperature is surely higher than the gas temperature. Our relatively short reactor length of 32 mm also increases the effect of temperature drop at both ends of the heated zone, and we have no measurement of this magnitude. However, it is reasonable to conclude that our effective true gas temperature is lower than our externally measured value, and that this error (arising from heat loss, which is proportional to the temperature gap between the heated zone and the unheated surroundings) becomes larger as temperature increases. As a result, all of our experimental data points in Fig. 4(b) should be shifted to the left (to lower temperatures), with the magnitude of this shift increasing with temperature. Such a shift would improve the agreement with the ME predictions for all isomers except benzene. However, our largest disagreements with the ME occur in the 600–675 K range, whereas this source of systematic error should require the largest shifts at the highest temperatures. Therefore our temperature errors cannot be the only source of theory/experiment disagreement, though they surely contribute.

Stein et al. used more dilute concentrations of 1,5-HD than did we, delivering 1,5-HD at 0.002-0.080%, whereas our mole fraction of 1,5-HD delivered to the reactor could be as high as 2.5%. They found little dependence on 1,5-HD concentration, except at their highest temperatures, which are higher than ours. Nevertheless, all the experiments are fairly dilute, and given that Stein et al. found no evidence for free radical reactions, it isn't clear that these differences in concentration would have any systematic effect.

Finally, Stein et al. used gas chromatography to disperse different isomers according to their retention times on a chromatography column. This relatively slow method and the required high surface contact area needed for good chromatographic separation could have allow surface-catalyzed conversion of less stable to more stable isomers. We have no way of evaluating the likelihood of such surface-catalyzed conversions, but if they happened, the thermodynamic driving force for conversion to more stable isomers would lead to additional conversion of 1,5-HD to DMCB beyond what would be expected from pure gas-phase thermal isomerisation. Of course our experiments could also be distorted by surface-catalyzed conversion in our borosilicate reactor, but given our shorter residence times and the nearly instantaneous separation/detection method provided by PEPICO spectroscopy, we should be less susceptible to such systematic errors.

In summary, variations in residence time lead to fairly small shifts of mole fraction profiles by an amount that is nearly independent of temperature, which cannot account for the first and second discrepancies between the two experimental data sets shown in Fig. S4. Compared to Stein et al., our experiments likely have greater systematic error due to overestimation of the true gas temperature, but this error alone cannot explain our disagreement with the MK master equation model profiles. Concentration of the starting material is unlikely to cause significant errors. In our estimation, the systematic error that could have the largest effect on the Stein et al. data is the possibility of surface-catalyzed conversion to more stable isomers during the slow chromatography step of their work.

5.2 Insights into the reaction mechanism

Early theoretical calculations of the C_6H_6 PES by Miller and Melius,[7] for the purpose of studying the propargyl self reaction, found that benzene could only be formed through fulvene as a reaction intermediate. The most important conclusion Stein et al.[13] drew from their observation that fulvene and benzene appeared at the same temperature is that there must be parallel pathways from DMCB to fulvene and benzene. The later calculations of Miller and Klippenstein[12] found such parallel pathways. We depict in Fig. 5 the portions of their PES that are relevant to the present experiments. To aid in understanding, we label five different parts of the PES as paths 1–5 and depict them in contrasting colours, adopting the numbering conventions of MK for the wells and saddle points.

Path 1 in black describes conversion of the reactant, 1,5-HD (**1**) by a (3,3) sigmatropic rearrangement into 1245-HT (**2**). Our inability to see any experimental evidence for this isomer is consistent with the ME predictions, which find that for temperatures high enough that 1245-HT forms, it rapidly converts to DMCB (**3**) via a (2,2) sigmatropic rearrangement enabled by the low barrier (**2–3**). However, DMCB itself is a dead-end for further isomerisation. At moderate temperatures, the equilibrium between 1245-HT and DMCB favors DMCB due to its lower enthalpy. However, as temperature increases, the low entropy of the rigid DMCB isomer favors conversion back to 1245-HT. It is from this isomer that paths 2 (red) and 4 (blue) lead to more stable isomers.

Path 4 is the lowest enthalpy exit from 1245-HT, leading to a carbene with a five-membered ring (**A**) that rapidly converts to fulvene (**4**). In competition, path 2 has a slightly higher barrier (**2–8**) that leads to 13HD5Y (**8**), which is the same isomer that is a minor impurity in our 1,5-HD sample. From 13HD5Y, both paths 2 (red) and 3 (green) connect to benzene (**7**) without going through fulvene. From 13HD5Y (**8**), the lower barriers of path 2 make it more favorable than path 3. Finally, path 5 enables the direct conversion of fulvene to benzene. However, the large energy difference between fulvene and its isomerisation barrier (**4–9**) means that, in the high-pressure limit, where equilibrium is established rapidly compared to chemical rearrangements, path 5 is completely negligible for $T < 1200$ K. Hence, the parallel paths 2 (forming fulvene) and 4 (forming benzene) are expected to dominate at the temperatures in this work.

Returning to the comparison of our experimental mole fractions with the MK model in Fig. 4(b), notice that the agreement for $T > 690$ K is reasonably good, whereas significant discrepancies exist for $T < 670$ K. Adjusting for the experimental temperature error discussed in section 5.1 would move our data points to lower temperature, but this correction could not improve agreement across all temperatures, as discussed in section 5.1. Instead, we ran an additional ME simulation with barrier (**1–2**) increased by 1.0 kcal mol^{-1}. These simulations are shown as dashed lines in Fig. 4(b) for all species. Note that the 1,5-HD profile and the rising edge of the DMCB

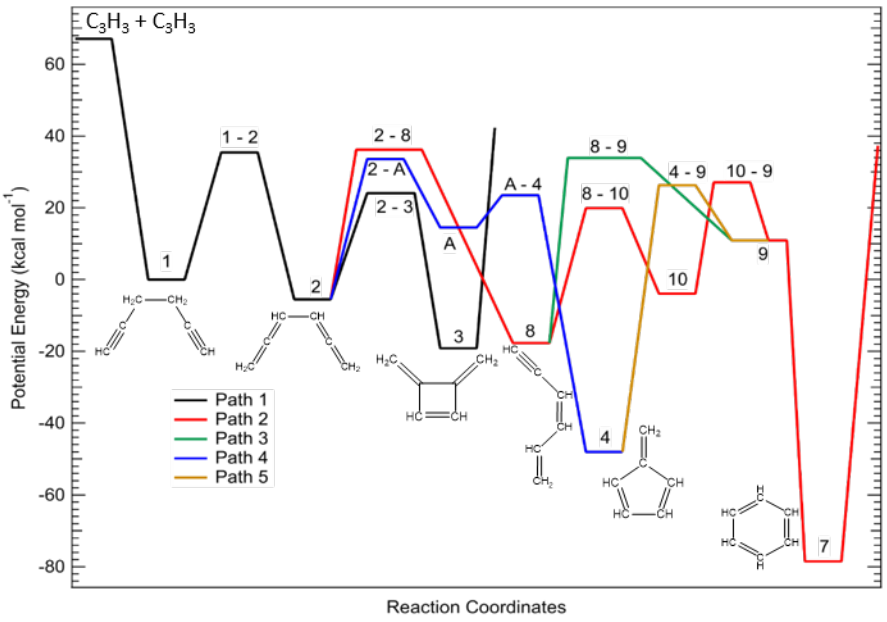

Fig. 5 Stationary points on the C_6H_6 potential energy surface. Numbering of wells and saddle points follows the conventions of Miller and Klippenstein.[12] See text for pathway descriptions.

profile are shifted to higher temperatures, improving agreement with experiment, whereas this change has no effect for T > 660 K. That dependence is expected because the conversion of DCMB to fulvene and benzene depends on barriers (**2–8**) and (**2–A**), which we left unchanged. Further increase in the energy of the barrier (**1–2**) would provide some additional improvement, but might not be justified considering that MK already increased the energy of this barrier by 1.0 kcal mol^{-1} to improve agreement with the data of Stein et al. Raising this barrier further would also not correct the different slopes of the the ME vs. experimental profiles of 1,5-HD and DMCB. We do not have a complete solution to this discrepancy.

Regarding the onset of fulvene and benzene, we note that the MK model clearly predicts that fulvene should have a lower-temperature onset compared to benzene, due to the lower barrier in path 4 compared to path 2 on the PES. Our experiments confirm this prediction, but take nothing away from the significant impact of the Stein et al.[13] experiments, which helped catalyze the theoretical search for independent routes to fulvene and benzene.

This work shows that rapid analysis of thermal isomerisation by PEPICO spectroscopy is possible even when five isomers contribute to the spectra, and despite the fact that some of the reference spectra required for extracting mole fractions from the data were not obtainable from pure chemical samples. Further development of methods, both theoretical[49] and experimental,[50] for the evaluation of photoionisation and integral TPE cross sections when authentic samples are not available will be important to improve the accuracy of PEPICO for this type of study.

6 Conclusions

We measured the thermal isomerisation of the least stable C_6H_6 isomer, 1,5-hexadiyne, in the 573–773 K temperature range via threshold photoelectron spectra obtained with photoelectron photoion coincidence spectroscopy. 1,5-hexadiyne isomerises to an equilibrated mixture of 1,2,4,5-hexatetrane and 3,4-dimethylenecyclobut-1-ene, where equilibrium favors the latter isomer. With increasing temperature, the very small steady-state concentration of 1,2,4,5-hexatetrane isomerises via parallel paths to fulvene and benzene. Our results are generally in agreement with prior experiments of Stein et al.,[13] although there are quantitative differences. Most importantly, they observe conversion to fulvene and benzene at the same temperature, whereas we clearly detect fulvene at 673 K, with benzene first appearing at 723 K. This spread in temperature onset was predicted by the RRKM-master equation simulations of Miller and Klippenstein.[12] Our experiments and master equation calculations confirm their electronic structure calculations, which show a lower energy rate-limiting barrier for the path to fulvene compared to the higher energy rate-limiting barrier on the path to benzene.

Despite the spectral congestion caused by the presence of five C_6H_6 isomers, threshold photoelectron spectra can provide isomer identification and quantification, and do so rapidly compared to other methods for isomer separation. This capability should make it a valuable tool for the future study of isomerisation mechanisms in closed- and open-shell molecular systems.

Conflicts of interest

There are no conflicts to declare.

Acknowledgements

J.Z. is grateful to Jim Miller for making his C_6H_6 master equation model available to her. We dedicate the paper to his memory. Experiments were carried out at the VUV beamline of the Swiss Light Source of the Paul Scherrer Institute. This material is based upon work supported by the Division of Chemical Sciences, Geosciences and Biosciences, Office of Basic Energy Sciences, USDOE. Sandia National Laboratories is a multimission laboratory managed and operated by National Technology and Engineering Solutions of Sandia, LLC, a wholly owned subsidiary of Honeywell International, Inc., for USDOE's National Nuclear Security Administration under Contract DE-NA-0003525. This paper describes objective technical results and analysis. Any subjective views or opinions that might be expressed in the paper do not necessarily represent the views of USDOE or the United States Government. B.Sz. was supported by the National Science Foundation (Grant CHE-1665464) A.B. and P.H acknowledge financial support by the Swiss Federal Office of Energy (SFOE) under grant number: SI/501269-01.

Notes and references

1 G. Wald, *Science*, 1968, **162**, 230–239.
2 J. Toullec, *Adv. Phys. Org. Chem.*, Elsevier, 1982, pp. 1–77.
3 A. C. Cope and E. M. Hardy, *J. Am. Chem. Soc.*, 1940, **62**, 441–444.
4 R. Breslow, *Tetrahedron Lett.*, 1959, **1**, 22–26.
5 M. F. Shaw, B. Sztáray, L. K. Whalley, D. E. Heard, D. B. Millet, M. J. T. Jordan, D. L. Osborn and S. H. Kable, *Nat. Commun.*, 2018, **9**, 2584.
6 M. F. Vansco, R. L. Caravan, S. Pandit, K. Zuraski, F. A. F. Winiberg, K. Au, T. Bhagde, N. Trongsiriwat, P. J. Walsh, D. L. Osborn, C. J. Percival, S. J. Klippenstein, C. A. Taatjes and M. I. Lester, *Phys. Chem. Chem. Phys.*, 2020, **22**, 26796–26805.
7 J. A. Miller and C. F. Melius, *Combust. Flame*, 1992, **91**, 21–39.
8 F. A. Lindemann, S. Arrhenius, I. Langmuir, N. R. Dhar, J. Perrin and W. C. M. Lewis, *Trans. Faraday Soc.*, 1922, **17**, 598–606.
9 H. Hopf, *Chem. Ber.*, 1971, **104**, 1499–1506.
10 C. H. Wu and R. D. Kern, *J. Phys. Chem.*, 1987, **91**, 6291–6296.
11 R. D. Kern, H. J. Singh and C. H. Wu, *Int. J. Chem. Kinet.*, 1988, **20**, 731–747.
12 J. A. Miller and S. J. Klippenstein, *J. Phys. Chem. A*, 2003, **107**, 7783–7799.
13 S. E. Stein, J. A. Walker, M. M. Suryan and A. Fahr, *Symp. Combust. Proc.*, 1991, **23**, 85–90.
14 J. Zádor, A. W. Jasper and J. A. Miller, *Phys. Chem. Chem. Phys.*, 2009, **11**, 11040.
15 T. A. Cool, K. Nakajima, T. A. Mostefaoui, F. Qi, A. McIlroy, P. R. Westmoreland, M. E. Law, L. Poisson, D. S. Peterka and M. Ahmed, *J. Chem. Phys.*, 2003, **119**, 8356–8365.
16 C. A. Taatjes, N. Hansen, D. L. Osborn, K. Kohse-Höinghaus, T. A. Cool and P. R. Westmoreland, *Phys. Chem. Chem. Phys.*, 2008, **10**, 20–34.
17 F. Qi, *Proc. Combust. Inst.*, 2013, **34**, 33–63.
18 A. Bodi, P. Hemberger, T. Gerber and B. Sztáray, *Rev. Sci. Instrum.*, 2012, **83**, 083105.
19 G. A. Garcia, B. K. C. de Miranda, M. Tia, S. Daly and L. Nahon, *Rev. Sci. Instrum.*, 2013, **84**, 053112.
20 X. Tang, G. A. Garcia, J.-F. Gil and L. Nahon, *Rev. Sci. Instrum.*, 2015, **86**, 123108.
21 B. Sztáray, K. Voronova, K. G. Torma, K. J. Covert, A. Bodi, P. Hemberger, T. Gerber and D. L. Osborn, *J. Chem. Phys.*, 2017, **147**, 013944.
22 T. Baer and R. P. Tuckett, *Phys. Chem. Chem. Phys.*, 2017, **19**, 9698–9723.
23 P. Hemberger, J. A. van Bokhoven, J. Pérez-Ramírez and A. Bodi, *Catal. Sci. Technol.*, 2020, **10**, 1975–1990.
24 P. Hemberger, A. Bodi, T. Bierkandt, M. Kohler, D. Kaczmarek and T. Kasper, *Energy Fuels*, 2021, **20**, 16265–16302.
25 M. Johnson, A. Bodi, L. Schulz and T. Gerber, *Nucl. Instrum. Methods Phys. Res., Sect. A*, 2009, **610**, 597–603.
26 A. Bodi, M. Johnson, T. Gerber, Z. Gengeliczki, B. Sztáray and T. Baer, *Rev. Sci. Instrum.*, 2009, **80**, 034101.
27 B. Sztáray and T. Baer, *Rev. Sci. Instrum.*, 2003, **74**, 3763–3768.
28 A. Bodi, B. Sztáray, T. Baer, M. Johnson and T. Gerber, *Rev. Sci. Instrum.*, 2007, **78**, 084102.
29 M. J. Frisch, G. W. Trucks, H. B. Schlegel, G. E. Scuseria, M. A. Robb, J. R. Cheeseman, G. Scalmani, V. Barone, G. A. Petersson, H. Nakatsuji, X. Li, M. Caricato, A. V. Marenich, J. Bloino, B. G. Janesko, R. Gomperts, B. Mennucci, H. P. Hratchian, J. V. Ortiz, A. F. Izmaylov, J. L. Sonnenberg, D. Williams-Young, F. Ding, F. Lipparini, F. Egidi, J. Goings, B. Peng, A. Petrone, T. Henderson, D. Ranasinghe, V. G. Zakrzewski, J. Gao, N. Rega, G. Zheng, W. Liang, M. Hada, M. Ehara, K. Toyota, R. Fukuda, J. Hasegawa, M. Ishida, T. Nakajima, Y. Honda, O. Kitao, H. Nakai, T. Vreven, K. Throssell, J. A. Montgomery, Jr., J. E. Peralta, F. Ogliaro, M. J. Bearpark, J. J. Heyd, E. N. Brothers, K. N. Kudin, V. N. Staroverov, T. A. Keith, R. Kobayashi, J. Normand, K. Raghavachari, A. P. Rendell, J. C. Burant, S. S. Iyengar, J. Tomasi, M. Cossi, J. M. Millam, M. Klene, C. Adamo, R. Cammi, J. W. Ochterski, R. L. Martin, K. Morokuma, O. Farkas, J. B. Foresman and D. J. Fox, *Gaussian 16 Revision C.01*, 2016, Gaussian Inc. Wallingford CT.

30 R. J. Bartlett and M. Musiał, *Rev. Mod. Phys.*, 2007, **79**, 291–352.

31 Y. Shao, L. F. Molnar, Y. Jung, J. Kussmann, C. Ochsenfeld, S. T. Brown, A. T. Gilbert, L. V. Slipchenko, S. V. Levchenko, D. P. O'Neill, R. A. D. Jr, R. C. Lochan, T. Wang, G. J. Beran, N. A. Besley, J. M. Herbert, C. Y. Lin, T. V. Voorhis, S. H. Chien, A. Sodt, R. P. Steele, V. A. Rassolov, P. E. Maslen, P. P. Korambath, R. D. Adamson, B. Austin, J. Baker, E. F. C. Byrd, H. Dachsel, R. J. Doerksen, A. Dreuw, B. D. Dunietz, A. D. Dutoi, T. R. Furlani, S. R. Gwaltney, A. Heyden, S. Hirata, C.-P. Hsu, G. Kedziora, R. Z. Khalliulin, P. Klunzinger, A. M. Lee, M. S. Lee, W. Liang, I. Lotan, N. Nair, B. Peters, E. I. Proynov, P. A. Pieniazek, Y. M. Rhee, J. Ritchie, E. Rosta, C. D. Sherrill, A. C. Simmonett, J. E. Subotnik, H. L. W. III, W. Zhang, A. T. Bell, A. K. Chakraborty, D. M. Chipman, F. J. Keil, A. Warshel, W. J. Hehre, H. F. S. III, J. Kong, A. I. Krylov, P. M. W. Gill and M. Head-Gordon, *Phys. Chem. Chem. Phys.*, 2006, **8**, 3172–3191.

32 L. A. Curtiss, P. C. Redfern and K. Raghavachari, *J. Chem. Phys.*, 2007, **126**, 084108.

33 S. J. Klippenstein, A. F. Wagner, R. C. Dunbar, D. M. Wardlaw, S. H. Robertson and J. Miller, *VARIFLEX; v. 2.03*, 2008.

34 J. A. Miller and S. J. Klippenstein, *J. Phys. Chem. A*, 2003, **107**, 2680–2692.

35 F. Brogli, E. Heilbronner, J. Wirz, E. Kloster-Jensen, R. G. Bergman, K. P. C. Vollhardt and A. J. Ashe, *Helv. Chim. Acta*, 1975, **58**, 2620–2645.

36 S. Ikuta, K. Yoshihara, T. Shiokawa, M. Jinno, Y. Yokoyama and S. Ikeda, *Chem. Lett.*, 1973, **2**, 1237–1240.

37 H. Rosenstock, J. Dannacher and J. Liebman, *Radiat. Phys. Chem.*, 1982, **20**, 7–28.

38 P. Bischof, R. Gleiter, H. Hopf and F. T. Lenich, *J. Am. Chem. Soc.*, 1975, **97**, 5467–5472.

39 E. Heilbronner, R. Gleiter, H. Hopf, V. Hornung and A. D. Meijere, *Helv. Chim. Acta*, 1971, **54**, 783–794.

40 P. Hemberger, Z. Pan, A. Bodi, J. A. Bokhoven, T. K. Ormond, G. B. Ellison, N. Genossar and J. H. Baraban, *ChemPhysChem*, 2020, **21**, 2217–2222.

41 G. Nemeth, H. Selzle and E. Schlag, *Chem. Phys. Lett.*, 1993, **215**, 151–155.

42 A. Bodi, N. S. Shuman and T. Baer, *Phys. Chem. Chem. Phys.*, 2009, **11**, 11013.

43 A. J. Yencha, R. I. Hall, L. Avaldi, G. Dawber, A. G. McConkey, M. A. MacDonald and G. C. King, *Can. J. Chem.*, 2004, **82**, 1061–1066.

44 O. Kostko, K. Bravaya, A. Krylov and M. Ahmed, *Phys. Chem. Chem. Phys.*, 2010, **12**, 2860.

45 K. B. Bravaya, O. Kostko, S. Dolgikh, A. Landau, M. Ahmed and A. I. Krylov, *J. Phys. Chem. A*, 2010, **114**, 12305–12317.

46 M. Bobeldijk, W. van der Zande and P. Kistemaker, *Chem. Phys.*, 1994, **179**, 125–130.

47 S. Soorkia, A. J. Trevitt, T. M. Selby, D. L. Osborn, C. A. Taatjes, K. R. Wilson and S. R. Leone, *J. Phys. Chem. A*, 2010, **114**, 3340–3354.

48 E. Rennie, C. Johnson, J. Parker, D. Holland, D. Shaw and M. Hayes, *Chem. Phys.*, 1998, **229**, 107–123.

49 S. Gozem, A. O. Gunina, T. Ichino, D. L. Osborn, J. F. Stanton and A. I. Krylov, *J. Phys. Chem. Lett.*, 2015, **6**, 4532–4540.

50 M. Demireva, K. Au and L. Sheps, *Phys. Chem. Chem. Phys.*, 2020, **22**, 24649–24661.